

Observation of diffractive J/ψ production at the Fermilab Tevatron

The CDF Collaboration

(Submitted to Physical Review Letters)

T. Affolder,²³ H. Akimoto,⁴⁵ A. Akopian,³⁷ M. G. Albrow,¹¹ P. Amaral,⁸ D. Amidei,²⁵ K. Anikeev,²⁴ J. Antos,¹ G. Apollinari,¹¹ T. Arisawa,⁴⁵ A. Artikov,⁹ T. Asakawa,⁴³ W. Ashmanskas,⁸ F. Azfar,³⁰ P. Azzi-Bacchetta,³¹ N. Bacchetta,³¹ H. Bachacou,²³ S. Bailey,¹⁶ P. de Barbaro,³⁶ A. Barbaro-Galtieri,²³ V. E. Barnes,³⁵ B. A. Barnett,¹⁹ S. Baroiant,⁵ M. Barone,¹³ G. Bauer,²⁴ F. Bedeschi,³³ S. Belforte,⁴² W. H. Bell,¹⁵ G. Bellettini,³³ J. Bellinger,⁴⁶ D. Benjamin,¹⁰ J. Bensinger,⁴ A. Beretvas,¹¹ J. P. Berge,¹¹ J. Berryhill,⁸ A. Bhatti,³⁷ M. Binkley,¹¹ D. Bisello,³¹ M. Bishai,¹¹ R. E. Blair,² C. Blocker,⁴ K. Bloom,²⁵ B. Blumenfeld,¹⁹ S. R. Blusk,³⁶ A. Bocci,³⁷ A. Bodek,³⁶ W. Bokhari,³² G. Bolla,³⁵ Y. Bonushkin,⁶ K. Borras,³⁷ D. Bortoletto,³⁵ J. Boudreau,³⁴ A. Brandl,²⁷ S. van den Brink,¹⁹ C. Bromberg,²⁶ M. Brozovic,¹⁰ E. Brubaker,²³ N. Bruner,²⁷ E. Buckley-Geer,¹¹ J. Budagov,⁹ H. S. Budd,³⁶ K. Burkett,¹⁶ G. Busetto,³¹ A. Byon-Wagner,¹¹ K. L. Byrum,² S. Cabrera,¹⁰ P. Calafiura,²³ M. Campbell,²⁵ W. Carithers,²³ J. Carlson,²⁵ D. Carlsmith,⁴⁶ W. Caskey,⁵ A. Castro,³ D. Cauz,⁴² A. Cerri,³³ A. W. Chan,¹ P. S. Chang,¹ P. T. Chang,¹ J. Chapman,²⁵ C. Chen,³² Y. C. Chen,¹ M. -T. Cheng,¹ M. Chertok,⁵ G. Chiarelli,³³ I. Chirikov-Zorin,⁹ G. Chlachidze,⁹ F. Chlebana,¹¹ L. Christofek,¹⁸ M. L. Chu,¹ Y. S. Chung,³⁶ C. I. Ciobanu,²⁸ A. G. Clark,¹⁴ A. Connolly,²³ M. E. Convery,³⁷ J. Conway,³⁸ M. Cordelli,¹³ J. Cranshaw,⁴⁰ R. Cropp,⁴¹ R. Culbertson,¹¹ D. Dagenhart,⁴⁴ S. D'Auria,¹⁵ F. DeJongh,¹¹ S. Dell'Agnello,¹³ M. Dell'Orso,³³ L. Demortier,³⁷ M. Deninno,³ P. F. Derwent,¹¹ T. Devlin,³⁸ J. R. Dittmann,¹¹ A. Dominguez,²³ S. Donati,³³ J. Done,³⁹ M. D'Onofrio,³³ T. Dorigo,¹⁶ N. Eddy,¹⁸ K. Einsweiler,²³ J. E. Elias,¹¹ E. Engels, Jr.,³⁴ R. Erbacher,¹¹ D. Errede,¹⁸ S. Errede,¹⁸ Q. Fan,³⁶ R. G. Feild,⁴⁷ J. P. Fernandez,¹¹ C. Ferretti,³³ R. D. Field,¹² I. Fiori,³ B. Flaughner,¹¹ G. W. Foster,¹¹ M. Franklin,¹⁶ J. Freeman,¹¹ J. Friedman,²⁴ Y. Fukui,²² I. Furic,²⁴ S. Galeotti,³³ A. Gallas,^(**) 16 M. Gallinaro,³⁷ T. Gao,³² M. Garcia-Sciveres,²³ A. F. Garfinkel,³⁵ P. Gatti,³¹ C. Gay,⁴⁷ D. W. Gerdes,²⁵ P. Giannetti,³³ V. Glagolev,⁹ D. Glenzinski,¹¹ M. Gold,²⁷ J. Goldstein,¹¹ I. Gorelov,²⁷ A. T. Goshaw,¹⁰ Y. Gotra,³⁴ K. Goulianos,³⁷ C. Green,³⁵ G. Grim,⁵ P. Gris,¹¹ L. Groer,³⁸ C. Grosso-Pilcher,⁸ M. Guenther,³⁵ G. Guillian,²⁵ J. Guimaraes da Costa,¹⁶ R. M. Haas,¹² C. Haber,²³ S. R. Hahn,¹¹ C. Hall,¹⁶ T. Handa,¹⁷ R. Handler,⁴⁶ W. Hao,⁴⁰ F. Happacher,¹³ K. Hara,⁴³ A. D. Hardman,³⁵ R. M. Harris,¹¹ F. Hartmann,²⁰ K. Hatakeyama,³⁷ J. Hauser,⁶ J. Heinrich,³² A. Heiss,²⁰ M. Herndon,¹⁹ C. Hill,⁵ K. D. Hoffman,³⁵ C. Holck,³² R. Hollebeek,³² L. Holloway,¹⁸ R. Hughes,²⁸ J. Huston,²⁶ J. Huth,¹⁶ H. Ikeda,⁴³ J. Incandela,¹¹ G. Introzzi,³³ J. Iwai,⁴⁵ Y. Iwata,¹⁷ E. James,²⁵ M. Jones,³² U. Joshi,¹¹ H. Kambara,¹⁴ T. Kamon,³⁹ T. Kaneko,⁴³ K. Karr,⁴⁴ H. Kasha,⁴⁷ Y. Kato,²⁹ T. A. Keaffaber,³⁵ K. Kelley,²⁴ M. Kelly,²⁵ R. D. Kennedy,¹¹ R. Kephart,¹¹ D. Khazins,¹⁰ T. Kikuchi,⁴³ B. Kilminster,³⁶ B. J. Kim,²¹ D. H. Kim,²¹ H. S. Kim,¹⁸ M. J. Kim,²¹ S. B. Kim,²¹ S. H. Kim,⁴³ Y. K. Kim,²³ M. Kirby,¹⁰ M. Kirk,⁴ L. Kirsch,⁴ S. Klimenko,¹² P. Koehn,²⁸ K. Kondo,⁴⁵ J. Konigsberg,¹² A. Korn,²⁴ A. Korytov,¹² E. Kovacs,² J. Kroll,³² M. Kruse,¹⁰ S. E. Kuhlmann,² K. Kurino,¹⁷ T. Kuwabara,⁴³ A. T. Laasanen,³⁵ N. Lai,⁸ S. Lami,³⁷ S. Lammel,¹¹ J. Lancaster,¹⁰ M. Lancaster,²³ R. Lander,⁵ A. Lath,³⁸ G. Latino,³³ T. LeCompte,² A. M. Lee IV,¹⁰ K. Lee,⁴⁰ S. Leone,³³ J. D. Lewis,¹¹ M. Lindgren,⁶ T. M. Liss,¹⁸ J. B. Liu,³⁶ Y. C. Liu,¹ D. O. Litvintsev,¹¹ O. Lobban,⁴⁰ N. Lockyer,³² J. Loken,³⁰ M. Loret,³¹ D. Lucchesi,³¹ P. Lukens,¹¹ S. Lusin,⁴⁶ L. Lyons,³⁰ J. Lys,²³ R. Madrak,¹⁶ K. Maeshima,¹¹ P. Maksimovic,¹⁶ L. Malferrari,³ M. Mangano,³³ M. Mariotti,³¹ G. Martignon,³¹ A. Martin,⁴⁷ J. A. J. Matthews,²⁷ J. Mayer,⁴¹ P. Mazzanti,³ K. S. McFarland,³⁶ P. McIntyre,³⁹ E. McKigney,³² M. Menguzzato,³¹ A. Menzione,³³ C. Mesropian,³⁷ A. Meyer,¹¹ T. Miao,¹¹ R. Miller,²⁶ J. S. Miller,²⁵ H. Minato,⁴³ S. Miscetti,¹³ M. Mishina,²² G. Mitselmakher,¹² N. Moggi,³ E. Moore,²⁷ R. Moore,²⁵ Y. Morita,²² T. Moulik,³⁵ M. Mulhearn,²⁴ A. Mukherjee,¹¹ T. Muller,²⁰ A. Munar,³³ P. Murat,¹¹ S. Murgia,²⁶ J. Nachtman,⁶ V. Nagaslaev,⁴⁰ S. Nahn,⁴⁷ H. Nakada,⁴³ I. Nakano,¹⁷ C. Nelson,¹¹ T. Nelson,¹¹ C. Neu,²⁸ D. Neuberger,²⁰ C. Newman-Holmes,¹¹ C.-Y. P. Ngan,²⁴ H. Niu,⁴ L. Nodulman,² A. Nomerotski,¹² S. H. Oh,¹⁰ Y. D. Oh,²¹ T. Ohmoto,¹⁷ T. Ohsugi,¹⁷ R. Oishi,⁴³ T. Okusawa,²⁹ J. Olsen,⁴⁶ W. Orejudos,²³ C. Pagliarone,³³ F. Palmonari,³³ R. Paoletti,³³ V. Papadimitriou,⁴⁰ D. Partos,⁴ J. Patrick,¹¹ G. Pauletta,⁴² M. Paulini,^(*) 23 C. Paus,²⁴ D. Pellett,⁵ L. Pescara,³¹ T. J. Phillips,¹⁰ G. Piacentino,³³ K. T. Pitts,¹⁸ A. Pompos,³⁵ L. Pondrom,⁴⁶ G. Pope,³⁴ M. Popovic,⁴¹ F. Prokoshin,⁹ J. Proudfoot,² F. Ptohos,¹³ O. Pukhov,⁹ G. Punzi,³³ A. Rakitine,²⁴ F. Ratnikov,³⁸ D. Reher,²³ A. Reichold,³⁰ A. Ribon,³¹ W. Riegler,¹⁶ F. Rimondi,³ L. Ristori,³³ M. Riveline,⁴¹ W. J. Robertson,¹⁰ A. Robinson,⁴¹ T. Rodrigo,⁷ S. Rolli,⁴⁴ L. Rosenson,²⁴ R. Roser,¹¹ R. Rossin,³¹ A. Roy,³⁵ A. Ruiz,⁷ A. Safonov,⁵ R. St. Denis,¹⁵ W. K. Sakumoto,³⁶ D. Saltzberg,⁶ C. Sanchez,²⁸ A. Sansoni,¹³ L. Santi,⁴² H. Sato,⁴³ P. Savard,⁴¹ P. Schlabach,¹¹ E. E. Schmidt,¹¹ M. P. Schmidt,⁴⁷ M. Schmitt,^(**) 16 L. Scodellaro,³¹ A. Scott,⁶ A. Scribano,³³ S. Segler,¹¹ S. Seidel,²⁷ Y. Seiya,⁴³ A. Semenov,⁹ F. Semeria,³ T. Shah,²⁴ M. D. Shapiro,²³ P. F. Shepard,³⁴ T. Shibayama,⁴³ M. Shimojima,⁴³ M. Shochet,⁸ A. Sidoti,³¹ J. Siegrist,²³ A. Sill,⁴⁰ P. Sinervo,⁴¹ P. Singh,¹⁸ A. J. Slaughter,⁴⁷ K. Sliwa,⁴⁴ C. Smith,¹⁹ F. D. Snider,¹¹ A. Solodsky,³⁷ J. Spalding,¹¹ T. Speer,¹⁴ P. Sphicas,²⁴ F. Spinella,³³ M. Spiropulu,¹⁶ L. Spiegel,¹¹ J. Steele,⁴⁶ A. Stefanini,³³

J. Strologas,¹⁸ F. Strumia,¹⁴ D. Stuart,¹¹ K. Sumorok,²⁴ T. Suzuki,⁴³ T. Takano,²⁹ R. Takashima,¹⁷ K. Takikawa,⁴³ P. Tamburello,¹⁰ M. Tanaka,⁴³ B. Tannenbaum,⁶ M. Tecchio,²⁵ R. Tesarek,¹¹ P. K. Teng,¹ K. Terashi,³⁷ S. Tether,²⁴ A. S. Thompson,¹⁵ R. Thurman-Keup,² P. Tipton,³⁶ S. Tkaczyk,¹¹ D. Toback,³⁹ K. Tollefson,³⁶ A. Tollestrup,¹¹ D. Tonelli,³³ H. Toyoda,²⁹ W. Trischuk,⁴¹ J. F. de Troconiz,¹⁶ J. Tseng,²⁴ N. Turini,³³ F. Ukegawa,⁴³ T. Vaiciulis,³⁶ J. Valls,³⁸ S. Vejcek III,¹¹ G. Velez,¹¹ G. Veramendi,²³ R. Vidal,¹¹ I. Vila,⁷ R. Vilar,⁷ I. Volobouev,²³ M. von der Mey,⁶ D. Vucinic,²⁴ R. G. Wagner,² R. L. Wagner,¹¹ N. B. Wallace,³⁸ Z. Wan,³⁸ C. Wang,¹⁰ M. J. Wang,¹ B. Ward,¹⁵ S. Waschke,¹⁵ T. Watanabe,⁴³ D. Waters,³⁰ T. Watts,³⁸ R. Webb,³⁹ H. Wenzel,²⁰ W. C. Wester III,¹¹ A. B. Wicklund,² E. Wicklund,¹¹ T. Wilkes,⁵ H. H. Williams,³² P. Wilson,¹¹ B. L. Winer,²⁸ D. Winn,²⁵ S. Wolbers,¹¹ D. Wolinski,²⁵ J. Wolinski,²⁶ S. Wolinski,²⁵ S. Worm,²⁷ X. Wu,¹⁴ J. Wyss,³³ W. Yao,²³ G. P. Yeh,¹¹ P. Yeh,¹ J. Yoh,¹¹ C. Yosef,²⁶ T. Yoshida,²⁹ I. Yu,²¹ S. Yu,³² Z. Yu,⁴⁷ A. Zanetti,⁴² F. Zetti,²³ and S. Zucchelli³

¹ *Institute of Physics, Academia Sinica, Taipei, Taiwan 11529, Republic of China*

² *Argonne National Laboratory, Argonne, Illinois 60439*

³ *Istituto Nazionale di Fisica Nucleare, University of Bologna, I-40127 Bologna, Italy*

⁴ *Brandeis University, Waltham, Massachusetts 02254*

⁵ *University of California at Davis, Davis, California 95616*

⁶ *University of California at Los Angeles, Los Angeles, California 90024*

⁷ *Instituto de Fisica de Cantabria, CSIC-University of Cantabria, 39005 Santander, Spain*

⁸ *Enrico Fermi Institute, University of Chicago, Chicago, Illinois 60637*

⁹ *Joint Institute for Nuclear Research, RU-141980 Dubna, Russia*

¹⁰ *Duke University, Durham, North Carolina 27708*

¹¹ *Fermi National Accelerator Laboratory, Batavia, Illinois 60510*

¹² *University of Florida, Gainesville, Florida 32611*

¹³ *Laboratori Nazionali di Frascati, Istituto Nazionale di Fisica Nucleare, I-00044 Frascati, Italy*

¹⁴ *University of Geneva, CH-1211 Geneva 4, Switzerland*

¹⁵ *Glasgow University, Glasgow G12 8QQ, United Kingdom*

¹⁶ *Harvard University, Cambridge, Massachusetts 02138*

¹⁷ *Hiroshima University, Higashi-Hiroshima 724, Japan*

¹⁸ *University of Illinois, Urbana, Illinois 61801*

¹⁹ *The Johns Hopkins University, Baltimore, Maryland 21218*

²⁰ *Institut für Experimentelle Kernphysik, Universität Karlsruhe, 76128 Karlsruhe, Germany*

²¹ *Center for High Energy Physics: Kyungpook National University, Taegu 702-701; Seoul National University, Seoul 151-742; and SungKyunKwan University, Suwon 440-746; Korea*

²² *High Energy Accelerator Research Organization (KEK), Tsukuba, Ibaraki 305, Japan*

²³ *Ernest Orlando Lawrence Berkeley National Laboratory, Berkeley, California 94720*

²⁴ *Massachusetts Institute of Technology, Cambridge, Massachusetts 02139*

²⁵ *University of Michigan, Ann Arbor, Michigan 48109*

²⁶ *Michigan State University, East Lansing, Michigan 48824*

²⁷ *University of New Mexico, Albuquerque, New Mexico 87131*

²⁸ *The Ohio State University, Columbus, Ohio 43210*

²⁹ *Osaka City University, Osaka 588, Japan*

³⁰ *University of Oxford, Oxford OX1 3RH, United Kingdom*

³¹ *Universita di Padova, Istituto Nazionale di Fisica Nucleare, Sezione di Padova, I-35131 Padova, Italy*

³² *University of Pennsylvania, Philadelphia, Pennsylvania 19104*

³³ *Istituto Nazionale di Fisica Nucleare, University and Scuola Normale Superiore of Pisa, I-56100 Pisa, Italy*

³⁴ *University of Pittsburgh, Pittsburgh, Pennsylvania 15260*

³⁵ *Purdue University, West Lafayette, Indiana 47907*

³⁶ *University of Rochester, Rochester, New York 14627*

³⁷ *Rockefeller University, New York, New York 10021*

³⁸ *Rutgers University, Piscataway, New Jersey 08855*

³⁹ *Texas A&M University, College Station, Texas 77843*

⁴⁰ *Texas Tech University, Lubbock, Texas 79409*

⁴¹ *Institute of Particle Physics, University of Toronto, Toronto M5S 1A7, Canada*

⁴² *Istituto Nazionale di Fisica Nucleare, University of Trieste/ Udine, Italy*

⁴³ *University of Tsukuba, Tsukuba, Ibaraki 305, Japan*

⁴⁴ *Tufts University, Medford, Massachusetts 02155*

⁴⁵ *Waseda University, Tokyo 169, Japan*

⁴⁶ *University of Wisconsin, Madison, Wisconsin 53706*

Abstract

We report the first observation of diffractive $J/\psi(\rightarrow \mu^+\mu^-)$ production in $\bar{p}p$ collisions at $\sqrt{s}=1.8$ TeV. Diffractive events are identified by their rapidity gap signature. In a sample of events with two muons of transverse momentum $p_T^\mu > 2$ GeV/ c within the pseudorapidity region $|\eta| < 1.0$, the ratio of diffractive to total J/ψ production rates is found to be $R_{J/\psi} = [1.45 \pm 0.25]\%$. The ratio $R_{J/\psi}(x)$ is presented as a function of x -Bjorken. By combining it with our previously measured corresponding ratio $R_{jj}(x)$ for diffractive dijet production, we extract a value of 0.59 ± 0.15 for the gluon fraction of the diffractive structure function of the proton.

PACS number(s): 13.85.Ni

In the course of our studies of high energy $\bar{p}p$ interactions at the Fermilab Tevatron using the Collider Detector at Fermilab (CDF), we have observed a class of events incorporating both a hard (high transverse momentum) partonic scattering and the characteristic signature of single diffraction dissociation, namely a leading proton or antiproton and a forward rapidity gap, defined as the absence of particles in a forward pseudorapidity (η) [1] region. The rapidity gap in such “hard diffraction” processes is attributed to the exchange of a Pomeron [2], which in QCD is a gluon/quark color-singlet construct with the quantum numbers of the vacuum. Experiments on hard diffraction can be used to address the question of whether the Pomeron has a unique, factorizable partonic structure.

In four previous Letters, we reported results from diffractive W -boson [3], dijet [4], and b -quark [5] production obtained using the rapidity gap signature, and dijet production in association with a leading antiproton [6]. These results include measurements of the gluon fraction [4,5] and of the x_{ij} (Bjorken x) dependence of the diffractive structure function of the antiproton [6]. Comparisons with diffractive deep inelastic scattering data obtained at the DESY ep collider HERA revealed a severe breakdown of QCD factorization, expressed mainly as a suppression of a factor of ~ 10 of the overall normalization of the diffractive structure function at the Tevatron. A breakdown of factorization was also observed between the diffractive structure functions measured from dijet production in single diffraction and in double Pomeron exchange at the Tevatron [7]. In this Letter, we report a measurement of diffractive J/ψ production in $\bar{p}p$ collisions at $\sqrt{s}=1800$ GeV, $p\bar{p} \rightarrow p(\text{or } \bar{p}) + J/\psi + X$, and compare the J/ψ diffractive fraction with the results of our previous hard diffraction measurements to further characterize the observed breakdown of factorization.

The data used in this analysis were collected during 1994-95 and correspond to an integrated luminosity of 80 pb^{-1} . The technique we use to extract the diffractive signal is identical to that used in our previous studies. In a data sample satisfying selection requirements for J/ψ decaying into $\mu^+\mu^-$, we look for events with a rapidity gap in either of the two forward regions of the detector covering the pseudorapidity range $2.4 < |\eta| < 5.9$. We define a rapidity gap as the absence of hits in the beam-beam counters (BBC), which cover the region $3.2 < |\eta| < 5.9$, and the absence of calorimeter towers with energy above 1.5 GeV within $2.4 < |\eta| < 4.2$. The size of the calorimeter towers in this region is $\Delta\eta \times \Delta\phi = 0.1 \times 5^\circ$.

The detector components relevant to J/ψ selection are the silicon vertex detector (SVX), the vertex time projection chamber (VTX), the central tracking chamber (CTC), the central electromagnetic and hadronic calorimeters surrounding the CTC, and the central muon detectors. The J/ψ acceptance is limited by the muon detectors, which cover the region $|\eta| < 1.0$. The SVX provides spatial measurements in the r - ϕ plane with a track impact parameter resolution of $[13 + (40 \text{ GeV}/c)/p_T] \mu\text{m}$. The VTX is used primarily to measure the longitudinal position z of an event’s primary vertex, and the CTC provides momentum analysis for charged particles. The combined CTC/SVX transverse momentum resolution for charged particles is $\sigma_{p_T}/p_T = 0.0009p_T \oplus 0.0066$, where p_T is in GeV/ c . Details of the CDF detector components can be found in Ref. [8].

A three-level dimuon trigger system was used to select events with a pair of muon candidates [9]. At Level 1, the dimuon trigger selection required the presence of two radially aligned pairs of time-correlated hits in the muon chambers. Level 2 required that each pair of muon chamber hits match a track in the CTC found by the Central Fast Track (CFT) processor, which performed a partial reconstruction of all CTC tracks and determined the p_T with a momentum resolution of $\sigma_{p_T}/p_T^2 = 0.035 (\text{GeV}/c)^{-1}$. At Level 3, performed in software, events were required to contain two oppositely charged muon candidates with an invariant mass within $300 \text{ MeV}/c^2$ of the J/ψ mass of $3096.9 \text{ MeV}/c^2$ [10].

In addition to the J/ψ selection requirements used in previous CDF analyses [11], the following two requirements were imposed on the data: first, since the BBC information is used to tag rapidity gaps, only data for which there was no BBC coincidence requirement in the trigger were considered; and second, since additional interactions in

the same beam-beam crossing would most likely spoil a diffractive rapidity gap, only events with one reconstructed primary vertex were retained. In order to ensure that reconstructed muons were found in the kinematic region where the trigger is highly efficient, a minimum transverse momentum of 2 GeV/c was required for each muon candidate. For a precise vertex measurement, both muons were required to be reconstructed in the SVX detector. The dimuon invariant mass distribution for events passing the above requirements is shown in Figure 1a. The signal region, defined as the dimuon mass range of $3.05 \leq M_{\mu^+\mu^-} < 3.15$ GeV/c², contains 18910 events.

There are three sources of dimuons in the above J/ψ candidate event sample: (a) J/ψ 's directly produced in $p\bar{p}$ collisions, or resulting from decays of intermediate states which are sufficiently short-lived (*e.g.* from χ_c decays) so that their measured decay vertex cannot be distinguished from the primary event vertex; (b) J/ψ 's from B -hadron decays, and (c) background from processes for which the dimuon invariant mass falls accidentally in the J/ψ signal mass window; the latter includes dimuons from Drell-Yan production, double semileptonic b -decays, meson decays-in-flight, and residual hadrons that penetrate the calorimeter and are misidentified as muons. The first two sources contribute to the J/ψ invariant mass peak, while the last comprises the background under the peak. The fraction of background events in the signal region is evaluated by fitting the dimuon mass distribution with a sum of a Gaussian and a linear function. The fit yields a background fraction of $(6.5 \pm 0.1)\%$ within the signal region.

The fraction of J/ψ 's from B -hadron decays can be determined by fitting the proper decay length distribution, $c\tau$, using the appropriate function for each of the three dimuon components described above. However, because we do not fully reconstruct B decays, we use an approximation to $c\tau$ described in [11] and referred to as pseudo- $c\tau$. In the signal region, the fraction of background events is fixed at the value of 0.065, obtained from the dimuon mass fit, and the pseudo- $c\tau$ distribution is fitted using for the background a parametrization derived from the sidebands and appropriate parametrizations for the prompt and B decay dimuon components [9,11]. The pseudo- $c\tau$ distribution for the signal region is shown in Fig. 1b with the fit result superimposed. The fraction of J/ψ mesons from B -hadron decays obtained from the fit is $(16.8 \pm 0.4)\%$. The vertical line at 100 μm separates two regions: a “long-lived” region dominated by B decays, and a “short-lived” region mostly due to prompt J/ψ mesons. The short-lived region contains 15824 events, which are used in the analysis below. By numerically integrating the fitted B decay component in this region, the B -hadron decay contamination is found to be 3.3%.

As in our previous rapidity gap studies [3–5], the diffractive signal is evaluated by considering the number of BBC hits, N_{BBC} , versus the number of the adjacent forward calorimeter towers with energy above 1.5 GeV, N_{CAL} . Figure 2a shows the correlation between N_{BBC} and N_{CAL} . The multiplicity in this figure is for the side of the detector with the lower BBC hit multiplicity. The (0,0) bin, $N_{\text{BBC}} = N_{\text{CAL}} = 0$, contains 92 events. The excess of events in this bin is attributed to diffractive production. The non-diffractive content of the (0,0) bin is evaluated from the diagonal of Fig. 2a with $N_{\text{BBC}} = N_{\text{CAL}}$, shown in Fig. 2b. The non- J/ψ background in each bin of this plot, estimated by fitting the dimuon mass distribution to the sum of a Gaussian and a constant function, was subtracted from the number of J/ψ candidates prior to plotting, yielding 87.4 ± 9.7 J/ψ events in the (0,0) bin. An extrapolation to bin (0,0) of a linear fit to the data of bins (2,2) to (12,12) yields 19.9 ± 3.9 non-diffractive events. The events in the (0,0) bin will be referred to as “diffractive”. Figures 2c and 2d show the J/ψ transverse momentum and pseudorapidity distribution, respectively, for the diffractive and total event samples. In Fig. 2d the sign of the J/ψ pseudorapidity for events with a gap at positive η is reversed, so that the gap appears always on the left.

The number of diffractive events in the (0,0) bin must be corrected for the efficiency of requiring a single reconstructed primary vertex, $\varepsilon_{1\text{vtx}}^{\text{SD}}$, as well as for random BBC and forward calorimeter occupancy. The single-vertex requirement, which is used to reject events due to multiple interactions, also rejects single interaction events with extra vertices due to track reconstruction ambiguities. Removing the single-vertex requirement yields 15.4 more diffractive J/ψ events, resulting in $\varepsilon_{1\text{vtx}}^{\text{SD}} = 0.85$. For non-diffractive events, the efficiency of the single-vertex requirement, $\varepsilon_{1\text{vtx}}^{\text{ND}}$, was evaluated by comparing the ratio of single-vertex to all events with the ratio expected from the instantaneous luminosity. This comparison yielded $\varepsilon_{1\text{vtx}}^{\text{ND}} = 0.56 \pm 0.04$. Finally, from a study of a sample of events with no reconstructed primary vertex collected in random beam-beam crossings, the combined BBC and forward calorimeter occupancy was measured to be 0.20 ± 0.06 .

After correcting the data for the efficiency of the single-vertex requirement and for the forward detector occupancy, we obtain a diffractive to total J/ψ production ratio of $R_{J/\psi}^{\text{gap}} = (0.42 \pm 0.07)\%$. This ratio is based on diffractive events satisfying our rapidity gap definition. Therefore, it must be corrected for the rapidity gap acceptance, ε^{gap} , defined as the ratio of events in bin (0,0) to the total number of diffractive events satisfying the same J/ψ requirements and produced within a specified range of ξ , where ξ is the fractional momentum loss of the leading (anti)proton. The gap acceptance for $\xi < 0.1$ was calculated using the POMPYT Monte Carlo generator [13] followed by a detector simulation. For a Pomeron structure function of the form $\beta f(\beta) = 1/\beta$ [6], where β is the fraction of the momentum of the Pomeron carried by a parton, ε^{gap} was found to be 0.29. Dividing $R_{J/\psi}^{\text{gap}}$ by ε^{gap} yields a diffractive to total production ratio of $R_{J/\psi} = (1.45 \pm 0.25)\%$.

The ratio $R_{J/\psi}$ is larger than the corresponding ratio for diffractive b -quark production, $R_{b\bar{b}} = (0.62 \pm 0.25)\%$ [5], by

a factor of 2.34 ± 0.35 . As both J/ψ and b -quark production are mainly sensitive to the gluon content of the Pomeron, we examine whether the difference in the two ratios could be attributed to the different average x_{bj} values of the two measurements. Given the $x_{bj}^{-0.45}$ dependence of the diffractive structure function measured in dijet production [6], the double ratio $R_{\bar{b}b}^{J/\psi} \equiv R_{J/\psi}/R_{\bar{b}b}$ is expected to be equal to $(x_{bj}^{J/\psi}/x_{bj}^{\bar{b}b})^{-0.45}$. Since in these measurements we consider only central J/ψ or b -quark production, the ratio $x_{bj}^{J/\psi}/x_{bj}^{\bar{b}b}$ is approximately proportional to the ratio of the corresponding average p_T value for each process, which is ≈ 6 GeV/ c for the J/ψ (see Fig. 2c) and ≈ 36 GeV/ c for the b -quark (about three times the average p_T of the b -decay electron [5]). The expected value for $R_{\bar{b}b}^{J/\psi}$ is then $\approx (6/36)^{-0.45} = 2.2$, in agreement with the measured value of 2.34 ± 0.35 .

For a more direct study of the diffractive structure function, we restricted our analysis to events in which at least one jet was reconstructed. A jet is defined as a cluster of calorimeter towers within a cone size of $\Delta R \equiv (\Delta\eta^2 + \Delta\phi^2)^{1/2} = 0.7$ with a seed tower of $E_T > 1$ GeV. Since our diffractive J/ψ events have a rapidity gap in the region $2.4 \leq |\eta| \leq 5.9$, the core of the reconstructed jet for both diffractive and non-diffractive events is restricted to the region $|\eta| < 1.7$. The number of events passing this requirement is 8732.

Figure 3 shows distributions for the $J/\psi + jet$ event sample: (a) is the diagonal $(N_{\text{CAL}}, N_{\text{BBC}})$ distribution, equivalent to that of Fig. 1b, (b) the corrected $\xi_{p,\bar{p}}$ distribution for the (anti)proton on the side of the gap, evaluated using calorimeter and BBC information in a procedure described in Ref. [7], (c) the J/ψ transverse momentum, and (d) the azimuthal angle difference, $\phi = |\phi_{J/\psi} - \phi_{jet}|$, between the J/ψ and the highest E_T jet.

The x_{bj} of the parton in the (anti)proton participating in J/ψ production is evaluated using the equation $x_{bj}^{\pm} = p_T^{J/\psi}(e^{\pm\eta_{J/\psi}} + e^{\pm\eta_{jet}})/\sqrt{s}$, where the $+$ ($-$) sign stands for $p(\bar{p})$. In leading order QCD calculations, the ratio of diffractive to non-diffractive production is equal to the ratio of the corresponding structure functions. For J/ψ production, the ratio $R_{J/\psi}(x)$ per unit ξ was evaluated for the events in the region $0.01 < \xi < 0.03$ (see Fig. 3b) and is plotted in Fig. 4 along with the same ratio for dijet production, $R_{jj}(x)$, obtained from Ref. [6]. The structure function relevant to dijet production is $F_{jj}(x) \sim g(x) + \frac{4}{9}q(x)$ [6], where $g(x)$ and $q(x)$ are the gluon and quark densities in the proton and $\frac{4}{9}$ is a color factor. For J/ψ production, which is dominated by gg interactions, $R_{J/\psi}(x) \simeq g^D(x)/g(x)$. The ratio of $R_{jj}(x)$ to $R_{J/\psi}(x)$ is given by

$$R_{J/\psi}^{jj}(x) \equiv \frac{R_{jj}(x)}{R_{J/\psi}(x)} = \frac{1 + \frac{4}{9} \frac{q^D(x)}{g^D(x)}}{1 + \frac{4}{9} \frac{q(x)}{g(x)}} \quad (1)$$

where the superscript D is used to label the diffractive parton densities. Evaluating this ratio of ratios by integrating the x_{bj} distributions for R_{jj} and $R_{J/\psi}$ in the region $0.004 \leq x \leq 0.01$ (kinematic boundaries for full acceptance) yields $[R_{jj}(x)/R_{J/\psi}(x)]_{\text{exp}} = 1.17 \pm 0.27(\text{stat})$. Using this value in Eq. 1 and the ratio of $q(x)/g(x) = 0.274$ at $x = 0.0063$ and $Q = 6$ GeV calculated from the proton GRV98LO parton distribution functions [14], the gluon fraction of the diffractive structure function of the (anti)proton is found to be $f_g^D = 0.59 \pm 0.14(\text{stat}) \pm 0.06(\text{syst})$, where the systematic uncertainty includes in quadrature the uncertainties of all correction factors. This gluon fraction is consistent with the value 0.54 ± 0.15 obtained by combining the results of diffractive W , dijet, and b -quark production [5].

We thank the Fermilab staff and the technical staffs of the participating institutions for their vital contributions. This work was supported by the U.S. Department of Energy and National Science Foundation; the Italian Istituto Nazionale di Fisica Nucleare; the Ministry of Education, Science, Sports and Culture of Japan; the Natural Sciences and Engineering Research Council of Canada; the National Science Council of the Republic of China; the Swiss National Science Foundation; the A. P. Sloan Foundation; the Bundesministerium fuer Bildung und Forschung, Germany; the Korea Science and Engineering Foundation (KoSEF); the Korea Research Foundation; the Comision Interministerial de Ciencia y Tecnologia, Spain; the Max Kade Foundation; and the Ministry of Education, Science and Research of the Federal State Nordrhein-Westfalen of Germany.

[1] We use rapidity and pseudorapidity, η , interchangeably; $\eta \equiv -\ln(\tan\frac{\theta}{2})$, where θ is the polar angle of a particle with respect to the proton beam direction. The azimuthal angle is denoted by ϕ , and transverse energy is defined as $E_T = E \sin\theta$.

[2] See P.D.B. Collins, *An Introduction to Regge Theory and High Energy Physics* (Cambridge University Press, Cambridge 1977).

[3] F. Abe *et al.*, Phys. Rev. Lett. **78**, 2698 (1997).

- [4] F. Abe *et al.*, Phys. Rev. Lett. **79**, 2636 (1997).
- [5] T. Affolder *et al.*, Phys. Rev. Lett. **84**, 232 (2000).
- [6] T. Affolder *et al.*, Phys. Rev. Lett. **84**, 5043 (2000).
- [7] T. Affolder *et al.*, Phys. Rev. Lett. **85**, 4215 (2000).
- [8] F. Abe *et al.*, Nucl. Instrum. Methods Phys. Res., Sect. A **271**, 387 (1988); D. Amidei *et al.*, Nucl. Instrum. Methods Phys. Res., Sect. A **350**, 73 (1994); P. Azzi *et al.*, Nucl. Instrum. Methods Phys. Res., Sect. A **360**, 137 (1995).
- [9] A. Solodsky, Ph.D. thesis, Rockefeller University, 2001 (unpublished).
- [10] D. E. Groom *et al.*, Eur. Phys. J. C. **15**, 1 (2000).
- [11] F. Abe *et al.*, Phys. Rev. D **57**, 5382 (1998).
- [12] T. Sjöstrand, Comput. Phys. Commun. **82**, 74 (1994).
- [13] P. Bruni, A. Edin and G. Ingelman, Report No. DESY-95, DRAFT, ISSN 0418-9833;
<http://www3.tsl.uu.se/thep/pompyt/>
- [14] M. Glück, E. Reya and A. Vogt, Eur. Phys. J. **C5**, 461 (1998).

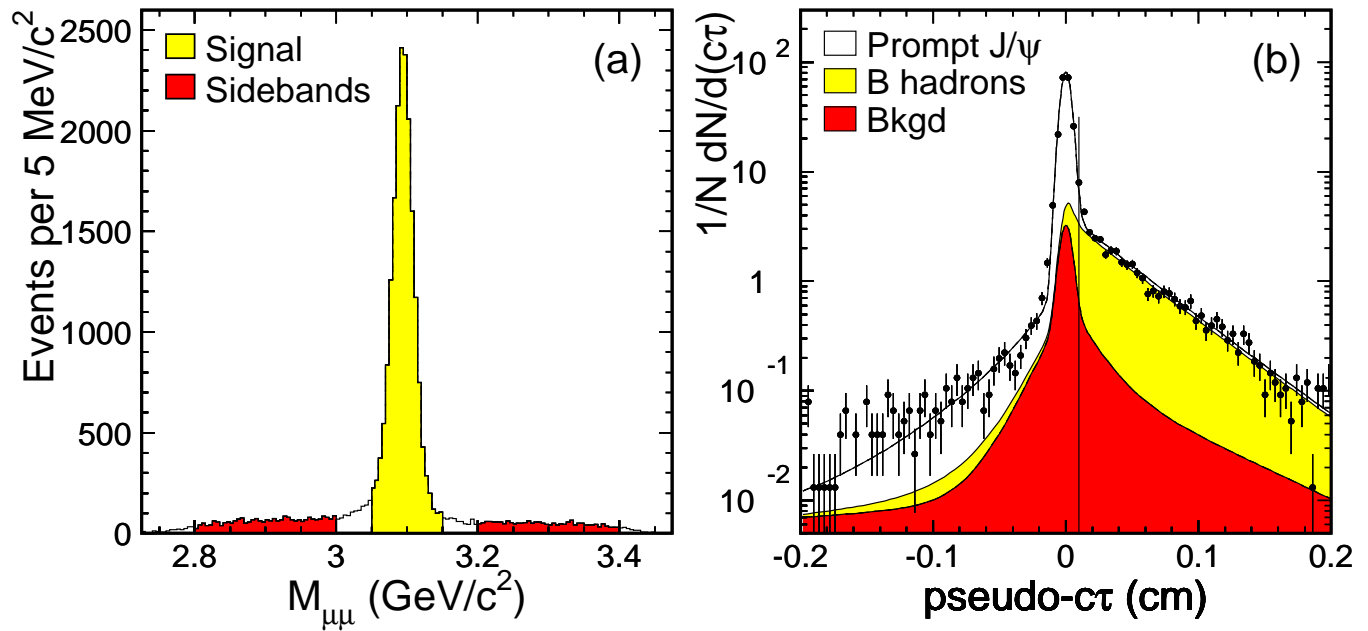


FIG. 1. (a) Dimuon invariant mass, and (b) pseudo- $c\tau$ for signal region with fit to the sum of contributions from prompt J/ψ production, J/ψ mesons from B -hadron decays and non- J/ψ background.

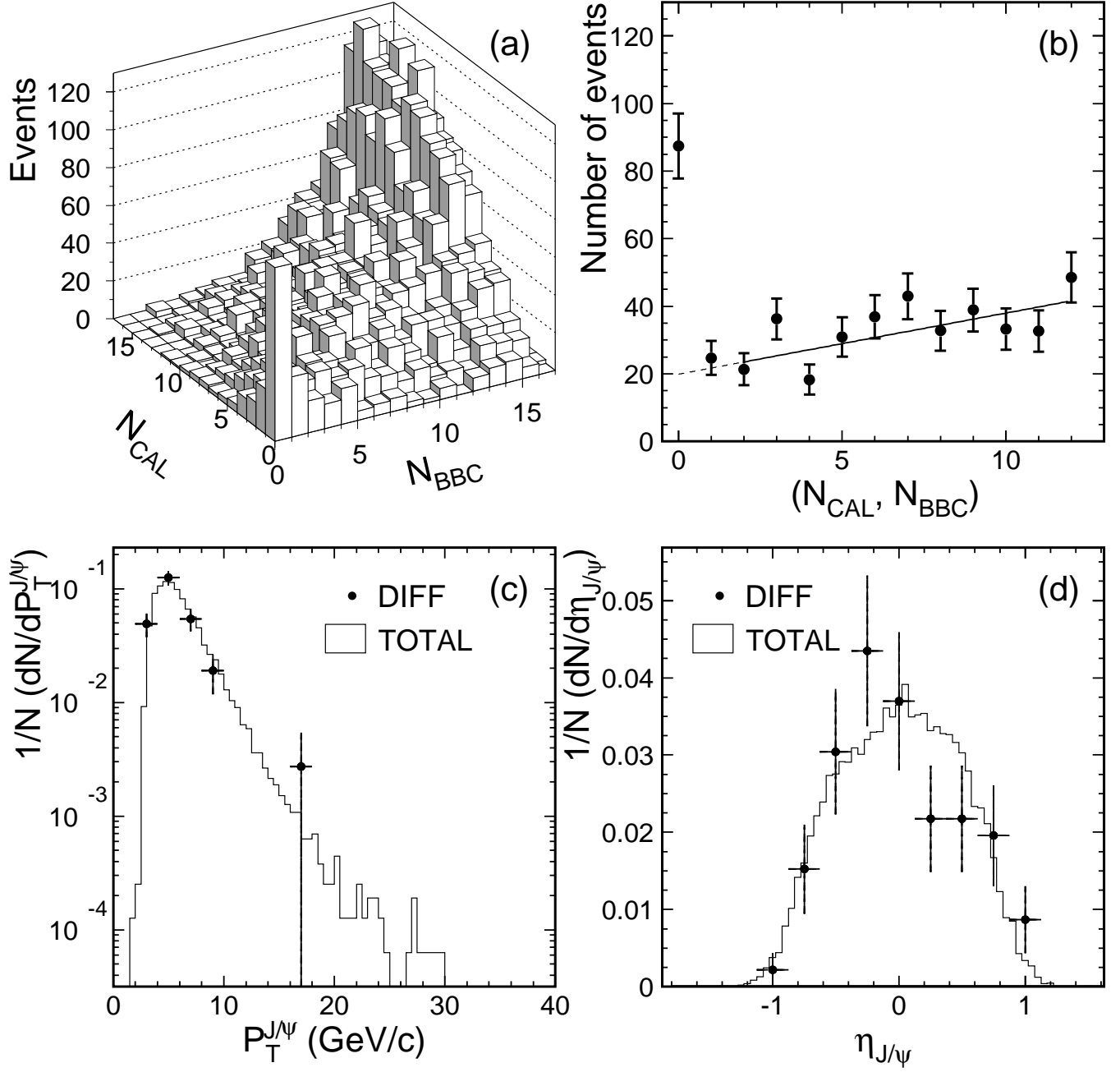


FIG. 2. J/ψ event sample distributions: (a) Beam-beam counter multiplicity, N_{BBC} , for the BBC with the lower multiplicity, versus forward calorimeter tower multiplicity, N_{CAL} ; (b) multiplicity distribution along the diagonal with $N_{\text{BBC}} = N_{\text{CAL}}$ in the plot of (a); (c) J/ψ transverse momentum and (d) J/ψ pseudorapidity.

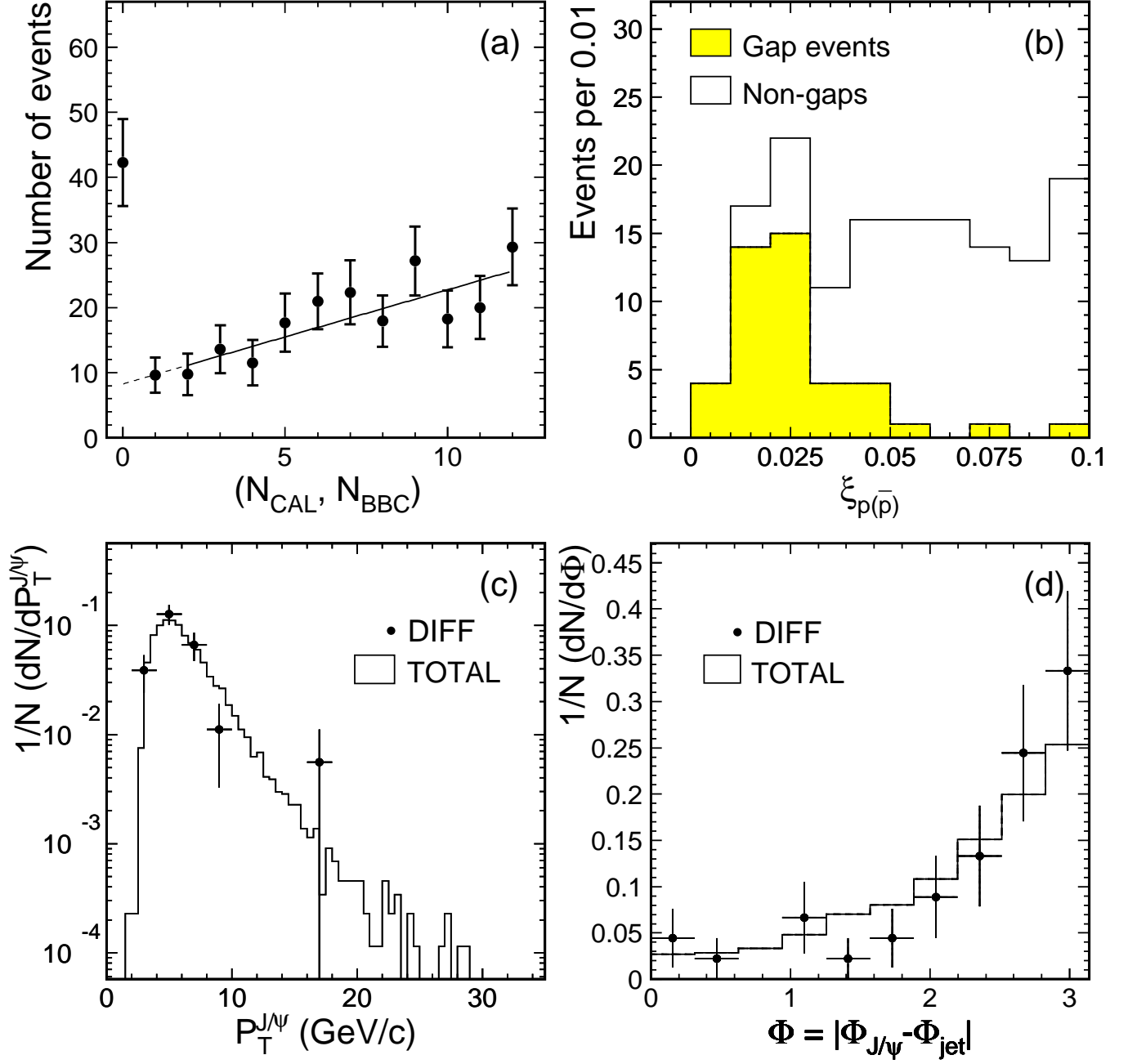


FIG. 3. Distributions for the $J/\psi + jet$ event sample: (a) the diagonal of the N_{BBC} versus N_{CAL} distribution with $N_{\text{BBC}} = N_{\text{CAL}}$; (b) Pomeron beam momentum fraction, $\xi_{p,\bar{p}}$ (corrected), for events with the J/ψ within $|\eta| < 1.1$ (the shaded area is the distribution for events satisfying the rapidity gap requirements); (c) J/ψ transverse momentum; (d) azimuthal angle difference between the J/ψ and the leading jet.

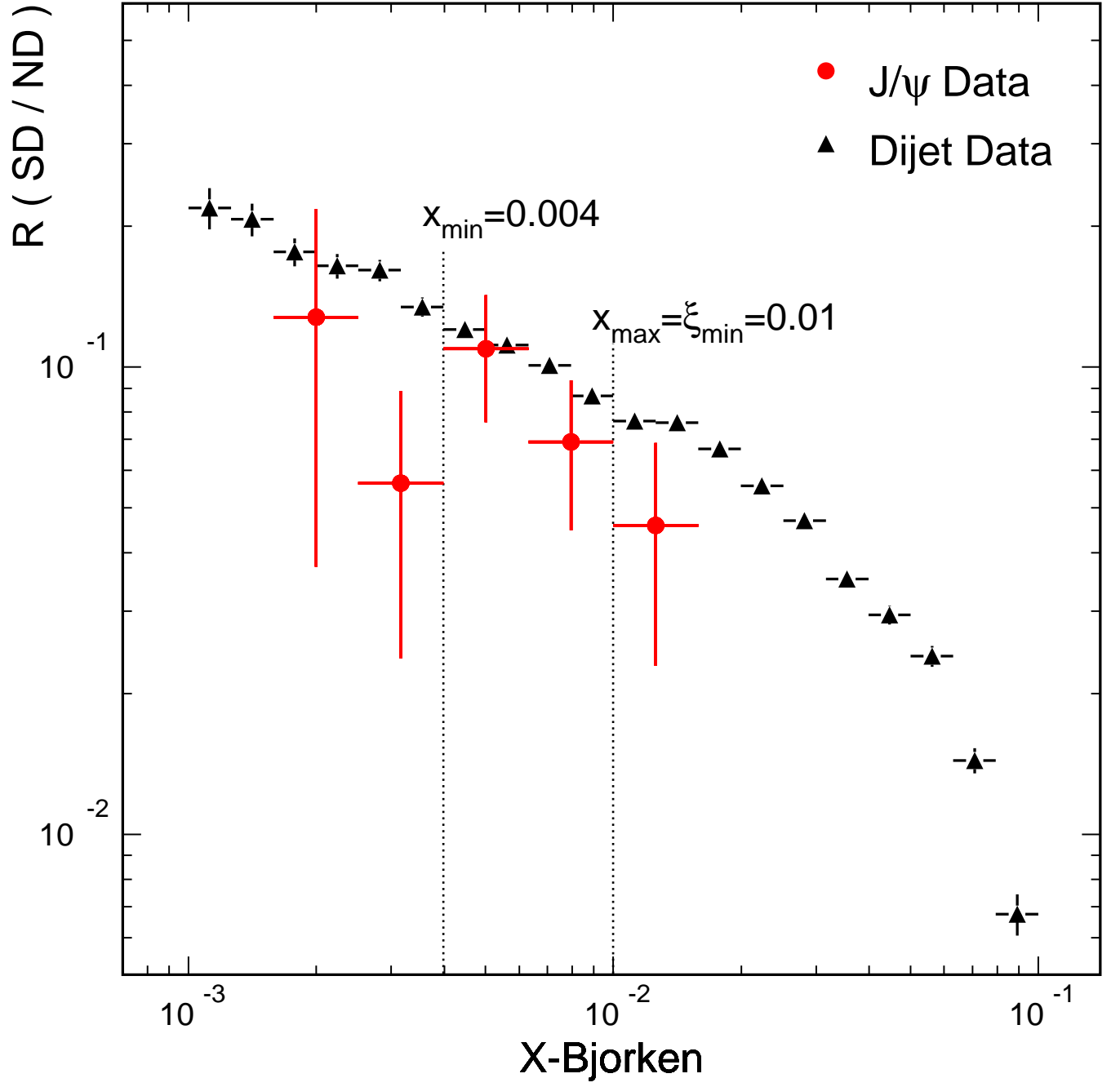


FIG. 4. Ratios of diffractive to non-diffractive J/ψ (circles) and dijet (triangles) rates per unit $\xi_p(\xi_{\bar{p}})$ as a function of x -Bjorken of the struck parton of the $p(\bar{p})$ adjacent to the rapidity gap.